

See discussions, stats, and author profiles for this publication at: <https://www.researchgate.net/publication/231392826>

Analysis of Finishing Reactive Distillation Columns

ARTICLE *in* INDUSTRIAL & ENGINEERING CHEMISTRY RESEARCH · NOVEMBER 1998

Impact Factor: 2.59 · DOI: 10.1021/ie9707073

CITATIONS

6

READS

17

4 AUTHORS, INCLUDING:



Pio Aguirre

Universidad Nacional del Litoral and Natio...

110 PUBLICATIONS 1,094 CITATIONS

SEE PROFILE

Analysis of Finishing Reactive Distillation Columns

José Espinosa,^{*,†} Pio Aguirre,[†] Thomas Frey, and Johann Stichlmair

Technische Universität München, Lehrstuhl A für Verfahrenstechnik, Boltzmannstrasse 15, 85748 Garching, Germany

In this paper, a novel method to deal with the design and the synthesis of finishing reactive distillation columns with one reactive core, two rectifying sections, and one stripping section is presented. The attention of our work is concentrated on three subjects: (i) the feasibility of a given separation at both finite and total reflux operation; (ii) the minimum energy demand operation; (iii) the distribution of the reaction between the reactor and the finishing reactive column. The design problem presents the same grade of difficulty as that found in the design of conventional extractive columns. A geometric based method is used to explain key features of reactive distillation. Here, the relation between the reaction yield and the distillate flow rate plays a role similar to that of the entrainer flow in extractive distillation. Hence, special attention is given to the behavior of the profiles inside the rectifying section below the reactive core. The methodology is illustrated using the well-known MTBE case study.

Introduction

Design and synthesis of reactive distillation columns are the subject of several works concentrating on mixtures with or without inerts, single or multiple equilibrium chemical reactions, reactive columns with catalyst on all stages, or columns with a reacting core. All the approaches to the design of reactive distillation consider the case of a feed stream entering the column at a stage containing catalyst.

In this paper we focus our attention on the design of a reactive column for the production of MTBE through the reaction between isobutene and methanol in the presence of butane as inert component. For this case and in line with the analysis developed by Bessling et al.¹ three sections are needed in order to produce high-purity MTBE. Pure rectifying and stripping sections are at both sides of the reactive part of the column. Thus, the combination of the reaction and the distillation in a single apparatus makes it possible to attain degrees of reagent conversion exceeding the thermodynamic equilibrium for the column operation conditions. Bessling et al.¹ used combined reactive and nonreactive distillation lines to determine the feasibility of the process under total reflux operation. These concepts can be employed to show that, at least for near total reflux operation, high-purity MTBE could be achieved at the bottom of the column independently of the feed stream location.

In our previous work (Espinosa et al.²) we demonstrated that high-purity MTBE can be achieved with the mentioned topology with the feed stream located inside the reactive core. However, we proved that this topology leads to a decomposition of MTBE at the end of the reactive core. Furthermore, the reaction was restricted to only a few trays near the feed tray and did not occur on all trays with catalyst, and finally, the range of reflux, for which a given separation can be achieved, is very small.

A better design is achieved with a column containing

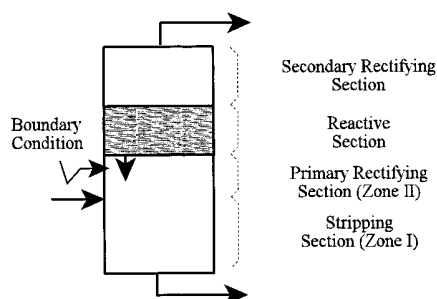


Figure 1. Reactive distillation column with a reacting core and three nonreactive zones.

one reactive core, two rectifying sections, and one stripping section. Figure 1 shows the topology to be studied, and Table 1 presents a comparative analysis of the previous and the new topology. To produce the same products from a given feed stream a different number of total stages results from the design calculations for each case.

Three major topics are covered: (1) the feasibility of a given separation at both finite and total reflux operation; (2) the minimum energy demand operation; (3) the distribution of the reaction between the reactor and the finishing reactive column. These subjects have significant impact on the design and the synthesis tasks.

Since the shape of the profiles in the rectifying section below the reactive core is determined by the presence of a saddle inside the tetrahedron, geometric based methods (Knapp and Doherty³) are used here to explain some key features of this quaternary single-feed reactive distillation. The ratio of the total number of moles reacted and the distillate flow rate (R/D) plays a similar role (but not the same) to the amount of entrainer in extractive distillation. Differences between extractive and reactive distillation are also highlighted in this paper.

This work is the continuation of a series of papers on an appropriate methodology for the design and synthesis of reactive distillation systems. The main bibliography concerning previous developments can be encountered in Espinosa et al.²

* To whom all correspondence should be addressed.

[†] Present address: INGAR, Avellaneda 3657, 3000 Santa Fe, Argentina.

Table 1. Comparison between the Two Column Topologies Considered in This Work

	new topology	previous topology
MTBE decomposn	not (+)	yes (-) (at the end of the reactive core)
distribution of the reactn through the trays with catalyst	gradual (+)	the reactn mainly occurs at the feed stage (-)
feasible region for given top and bottom products	broad (+)	narrow (-)
attainable products and conversion	high conversions and ether purity may be achieved (=)	high conversions and ether purity may be achieved (=)

Mathematical Model

To extend the methodology developed in previous papers (Espinosa et al.^{2,4}), we have to restate the mass balance equations for the different column sections. In this paper, the following topology is considered: a nonreactive stripping section is located at the end of the column. Also, there is a nonreactive primary rectifying section immediately above the stripping section. These two nonreactive sections are separated by the feed stream. The reaction occurs at the reactive core and above this zone a nonreactive secondary rectifying section is added. These zones are depicted in Figure 1.

In the following, we consider the case of a feed stream entering the column at some stage below the reactive part of the column. In addition we concentrate on the special case of finishing reactive distillation columns. A feed stream from a reactor is led to the reactive column where unconverted reactants, inerts, and products are separated and, at the same time, the limiting reagent conversion is almost fully achieved. The sequence of a fixed bed reactor and a reactive column facilitates the management of the heat of reaction effectively.

As we demonstrated in Espinosa et al.² even though the equilibrium reaction does not occur at all the column stages, it is possible to develop a model in terms of transformed variables for the entire column (i.e., mass balances around the column). This transformation is very advantageous because inlet and outlet product compositions are on a straight line through the feed composition. Therefore, the flow rates in the transformed field obey the lever arm rule. Note, however, that in this case the bottom represents a liquid composition at its boiling point with a MTBE mole fraction near unity. For the design the reactive quaternary mixture behaves like a nonreactive ternary mixture. Therefore, we use a similar procedure to specify the column. A detailed procedure is explained in a previous work (Espinosa et al.²). In this paper, we use the following liquid and vapor composition variables ($j = 1, nc - 1; j \neq k$) proposed in Espinosa et al.⁵

$$X_j = \frac{v_k X_j - v_j X_k}{v_k - v_j} \quad X_I = \frac{v_k X_I}{v_k - v_j} \quad (1)$$

$$Y_j = \frac{v_k Y_j - v_j Y_k}{v_k - v_j} \quad Y_I = \frac{v_k Y_I}{v_k - v_j} \quad (2)$$

Here I is the index of the nonreactive component.

The transformed model is also useful to compute the internal profiles inside the reactive section (in this case, the secondary rectifying section and the reactive core) until the reaction yield determined by the overall balance is achieved. At this point, the model reproduces the situation at the end of the reactive part. The liquid leaving the reactive zone must be in chemical equilibrium; this liquid stream also acts as a feed to the primary rectifying section. For a quaternary reacting system, this situation can be seen as the intersection

between a conventional primary rectifying profile and the reactive surface. Such an intersection is easily computed by using transformed compositions.

Once the overall balances are solved, the tray by tray procedure requires the selection of a value for the external reflux. Therefore, the internal profiles in the secondary rectifying section and in the reactive core can be calculated for the given reflux ratio until the reaction yield measured as the amount of limiting-reagent reacted is achieved. Thus, it is possible to compute the profiles inside the primary rectifying section since the mole fraction and flow rate at the end of the reactive core are known. Finally, a feasible design is reached when an intersection between the primary rectifying and stripping sections is found. The point of intersection determines the feed location. We briefly analyze here the equations that model both nonreactive stripping and primary rectifying sections of the reactive column. To derive the design equations we suppose (1) liquid boiling feed is present, (2) heat losses can be neglected, (3) the molar heat of phase change for the mixture is constant, (4) the heat of mixing can be neglected, (5) the heat capacity of the mixture is constant, (6) the reaction enthalpy change is negligible compared with the phase change enthalpy, (7) on each tray the equilibrium (phase equilibrium or phase-reaction equilibrium) is attained for the living streams, (8) the operating pressure is constant, and (9) the column operates with a partial condenser. As a consequence of the first seven assumptions, the energy and mass balances can be decoupled, and, hence, only the material balances and the equilibrium equations are used to compute the composition profiles for the column.

Tray by Tray Equations: Stripping Section (Zone I). This section includes all the trays from the partial reboiler to the feed stream tray. The plate to plate equations for this area are ($j = 1 - nc; n = 1 - N_{\text{stripping}}$)

$$x_{j,n+1} = \frac{s}{s+1} y_{j,n} + \frac{1}{s+1} x_{j,B} \quad (3)$$

where the external reboil ratio is defined as

$$s = \frac{V}{B} \quad (4)$$

V denotes the vapor flow rate along the column, and B denotes the bottom flow rate.

Tray by Tray Equations: Primary Rectifying Section (Zone II). This section includes all the trays from the feed tray to the last tray without catalyst. The plate to plate equations for the reagents, the product reaction, and the nonreactive component in this area are ($j = 1 - nc; n = [N_{\text{stripping}} + 1] - N_{\text{last}}$)

$$y_{j,m-1} = \frac{r}{r+1-v_{tD}} \bar{R}^{x_{j,m}} + \frac{1}{r+1-v_{tD}} \bar{R}^{y_{j,D}} - \frac{1}{r+1-v_{tD}} \bar{R}^{y_{j,D}} \quad (5)$$

The mass balance for the nonreactive species can be obtained by considering a stoichiometric coefficient for this component with a zero value.

Here, N_{last} represents the last tray without catalyst below the reactive core. Note that in eq 5 the index m is used to indicate that the calculations are performed from the top (more exactly from the boundary condition at the last reactive tray) downward. The reflux ratio in this section is defined by

$$r = \frac{L_{\text{II}}}{D} \quad (6)$$

In this equation, L_{II} represents the liquid flow rate in this section and D the distillate flow rate. Note that, in general, the liquid flow rate could change in the reactive part of the column due to the change in the total number of moles by chemical reaction. Therefore, L_{II} can differ from the liquid flow rate at the top of the column. This value can be obtained from the boundary condition at the last reactive tray of the column. In the same sense, a liquid composition in simultaneous chemical and vapor–liquid equilibrium should be used at the beginning of the calculations. The determination of whether we can begin with the calculation of the primary rectifying profile is easily accomplished once the reactive profile reaches a value for the reaction yield (measured as the ratio between the total number of moles reacted for any component and their respective stoichiometric coefficient; namely R) equals to that calculated through the overall balances.

It is clear that the tray by tray equations depend on a new parameter (the other is the reflux ratio): the ratio between the reaction yield R and the distillate flow rate D . The value of this ratio remains constant during the plate to plate calculations.

Note that eq 5 reproduces the situation of conventional distillation when the ratio R/D equals zero (i.e. no reaction occurs in the column). For this case, the limiting operating conditions of a column, the total reflux, and thermodynamically optimum operations act as limits of the all-possible adiabatic profiles departing from the distillate. On the other hand, by increase of the value of R/D a different pinch point curve and a different total reflux curve can be encountered. One of the topics of this work is to determine the influence of these limits on the feasibility of a given separation at finite values of the reflux ratio.

It is noteworthy that we can redefine the flow rate and the product compositions at the top of the column in order to apply the well-known algorithms for nonreactive distillation to determine the liquid profiles in the primary rectifying section. For this case the reflux is the ratio between the liquid flow rate L_{II} and the redefined distillate flow rate. Also, the algorithms to obtain pinch point curves can be computed as no reaction would take place. Liquid and vapor compositions in phase equilibrium will be aligned with the redefined distillate composition. The mentioned transformation is important from the algorithmic point of

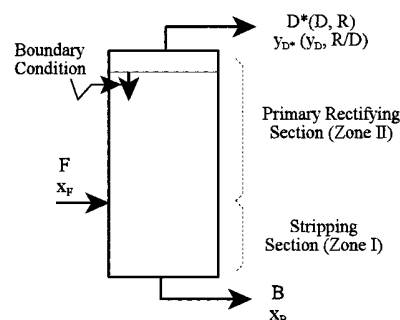


Figure 2. Hypothetical column representing the new model without chemical reaction.

view, since a minor number of corrections should be performed on the computational codes in order to obtain the new results. The redefined distillate compositions and flow rate are given by

$$y_{j,D}^{\text{new}} = \frac{y_{j,D} - v_{jD} \bar{R}}{1 - v_{tD} \bar{R}} \quad (7)$$

and

$$D^* = D - v_{tD} R \quad (8)$$

From eq 7 it is clear that some of the redefined product compositions could involve mole fractions with values lower than 0; therefore, this point acts as a “difference point”. The material balance line at any stage in the primary rectifying section points to the difference point. The location of the difference point has a deeper influence on the shape of the pinch point curve and, hence, on the feasibility of a given separation and on the shape of the internal profiles under minimum reflux. The problem appears to be similar to that of extractive distillation (Wahnschafft and Westerberg;⁶ Knapp and Doherty;³ Bauer and Stichlmair⁷), where a second feed is considered. Here, a number of hypothetical side streams (whose number equals the number of trays with catalyst) form an overall side stream with a component molar flow rate given by $-v_{jD} R$. In extractive distillation the “difference point” can be obtained by subtracting the entrainer stream from the distillate stream and represents the net flow from the stripping to the rectifying section. In reactive distillation, the “pole” is obtained by adding the distillate stream and the overall side stream (see eqs 7 and 8).

Figure 2 shows a hypothetical column that represents the new model without reaction. For a given overall mass balance, the feed and products are aligned for the case of a finite value of the reaction yield R , provided that the distillate mole fraction is calculated by means of eq 7.

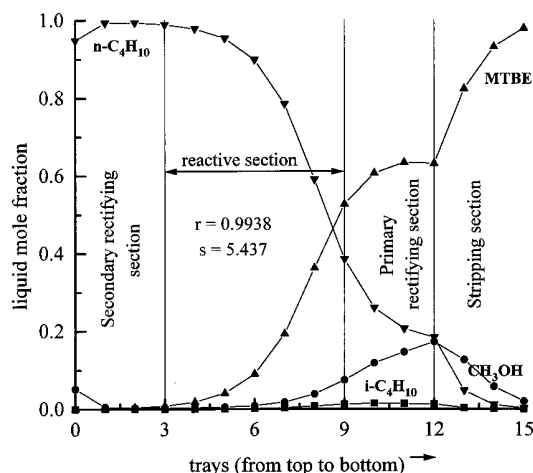
Example

We begin with the analysis of a base case in order to show the main characteristics of a reactive column that produces MTBE. Figure 3 shows the liquid profiles for a finishing column operating at 3 bar pressure and at a reflux ratio value of 0.9938. Table 2 presents the overall results for a feed stream that contains an excess of methanol and 20% mol/mol of MTBE. We have selected an operating pressure of 3 bar to promote high values

Table 2. Stream Results Corresponding to the Example

	flow rate	stream composns			
		isobutene	methanol	MTBE	<i>n</i> -butane
distillate	69.546	5.18×10^{-6}	0.051 712 63	0.000 094 83	0.948 187 36
feed	100.00	0.049 54	0.090 46	0.20	0.66
bottom	25.504	1.25×10^{-4}	0.019 571 48	0.978 053 53	2.25×10^{-3}

	flow rate	transformed variables		
		$X_{\text{isobutene}}$	X_{methanol}	$X_{\text{n-butane}}$
distillate	69.553	1.00×10^{-4}	0.051 80	0.948 10
feed	120.000	0.207 95	0.242 05	0.55
bottom	50.447	0.494 52	0.504 35	0.00113

**Figure 3.** Liquid profiles for the separation specified in Table 2.

of the chemical equilibrium constant. This selection was also made to generate an academic example despite the fact that an operating pressure near 8 bar is known to be the optimal value for this system. To obtain a feasible design we have to adjust the compositions of the two lower boiling components at the bottom product. As can be seen in Figure 3, the minimum boiling azeotrope between *n*-butane and methanol is obtained at the top of the column. The ether is mainly separated from the excess reagent at the stripping section. Immediately below the reactive part of the column the separation between the lighter and heavier components occurs. The inert is exhausted by distillation in the primary rectifying section and the stripping section of the column. Note that the limiting reactant isobutene is present in small amounts all along the column due to the reaction. The maximum concentration of isobutene is about 1.5 mol % and occurs at tray number 10 from the top. With this column topology, MTBE decomposition does not occur inside the reactive core. Moreover, a distribution of the reaction among the trays containing catalyst is accomplished.

Table 3 shows the compositions at the last tray with catalyst and the number of trays with catalyst required for different values of the external reflux ratio. The values of the table were obtained by computing the tray by tray procedure beginning at the distillate composition as was explained in our previous work (Espinosa et al.²). At a reflux value of 0.9307 eight trays with catalyst are needed, while at a reflux of 71.6 only one stage must contain the catalyst. Below of the lower bound for the energy demand, the reaction yield *R* calculated by means of the column overall balances is not accomplished. Above the upper bound, a fraction of an equilibrium stage is needed to achieve the reaction yield.

Table 3. Boundary Condition at the End of the Reactive Section for Different Values of the Reflux Ratio

example	reflux ratio	boilup	no. of trays	trays with catalyst
1	0.9307	5.2649	10	8
2	0.9938	5.4370	9	7
3	1.1280	5.8030	8	5
4	1.8625	7.8060	6	4
5	3.0270	10.9816	5	4
6	6.5250	20.5209	4	4
7	15.9000	46.0870	3	3
8	31.4250	88.4250	2	2
9	71.6000	197.9850	1	1

example	boundary condition at the end of the reactive core			
	isobutene	methanol	MTBE	<i>n</i> -butane
1	0.0140	0.1055	0.5830	0.2975
2	0.0123	0.0748	0.5269	0.3860
3	0.0104	0.0511	0.4513	0.4872
4	6.8010×10^{-3}	0.0170	0.2610	0.7152
5	5.1630×10^{-3}	6.8750×10^{-3}	0.1556	0.8324
6	3.5040×10^{-3}	1.9280×10^{-3}	0.0641	0.9305
7	1.9650×10^{-3}	4.9100×10^{-4}	0.0183	0.9792
8	7.2200×10^{-4}	3.4600×10^{-4}	5.9930×10^{-3}	0.9929
9	4.8000×10^{-5}	2.2920×10^{-3}	2.2660×10^{-3}	0.9954

Despite this, a value near 70 can be considered as a value near total reflux for all practical purposes. Therefore, these two values determine minimum and maximum values for the energy demand, in which the conversion yield can be accomplished.

Figure 4 presents the cumulative reaction versus the tray number for different values of the reflux ratio. The boundary condition at the end of the reactive zone was detected once the value of the reaction yield was equal to that calculated through the column overall balances. Since each of these curves has a maximum, the boundary condition must be selected in each case at the minimum number of trays for which the reaction yield is achieved. With this selection MTBE decomposition at the end of the reacting core is avoided.

Note that the minimum reflux for which the reaction yield is achieved not necessarily correspond to the minimum operation reflux. Although these values can coincide, the minimum operation reflux must be determined by intersection of the stripping and primary rectifying profiles.

Feasibility Criterion of a Given Separation

As it was explained by Wahnschafft et al.⁸ for the case of nonreactive mixtures, all the feasible composition profiles corresponding to the column products are enclosed by the corresponding reversible and total reflux profiles. For ternary systems both stripping and rectifying regions must overlap; therefore, there exists the possibility that, for a number of reflux and reboil ratios, the top and bottom profiles have a point in com-

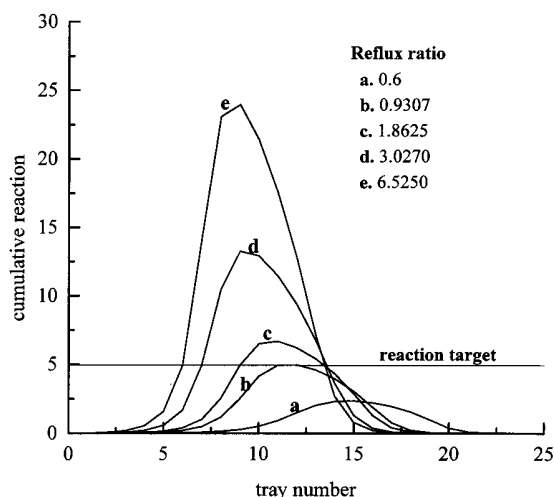


Figure 4. Cumulative reaction vs tray number for different values of the reflux ratio. (Separation specified in Table 2.)

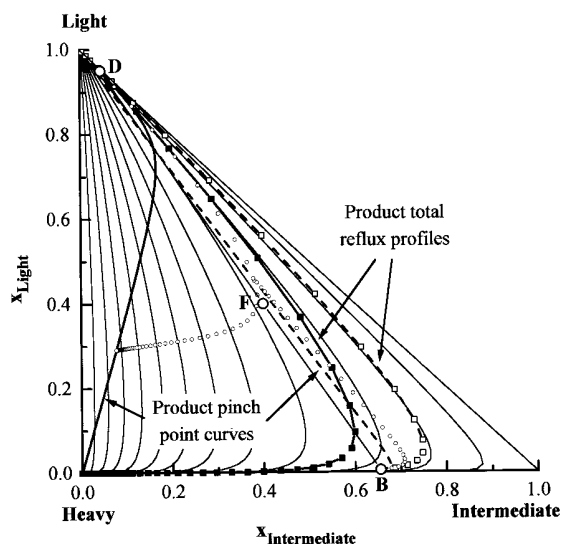


Figure 5. Feasibility of a given separation for finite values of the reflux ratio.

mon, i.e., the feed tray. The condition developed by Wahnschafft et al.⁸ is only necessary and exactly applicable to ternary mixtures. Figure 5 shows the feasibility criterion applied to the separation of a ternary nonreactive mixture F into a bottom B and a distillate D. The whole range of concentrations that could conceivably be covered by composition profiles of the rectifying section is enclosed by the total reflux curve through D and the pinch point curve for product D as it is shown in Figure 5. All possible concentrations profiles in the stripping section are confined by the total reflux curve and the pinch point curve for the bottom in question. For a feasible specification of products D and B, the liquid composition profiles of both column sections must meet somewhere in the region of overlap. Figure 5 shows that there exists a region of overlap for the selected product specification and, hence, the separation is in principle possible. This figure also shows the profiles under minimum reflux operation. An active pinch is found immediately below the feed tray. By analyzing the composition profiles in Figure 3, one can develop an approximate feasibility condition for the quaternary mixture because one of the reagents (isobutene) has a low liquid-phase composition through the

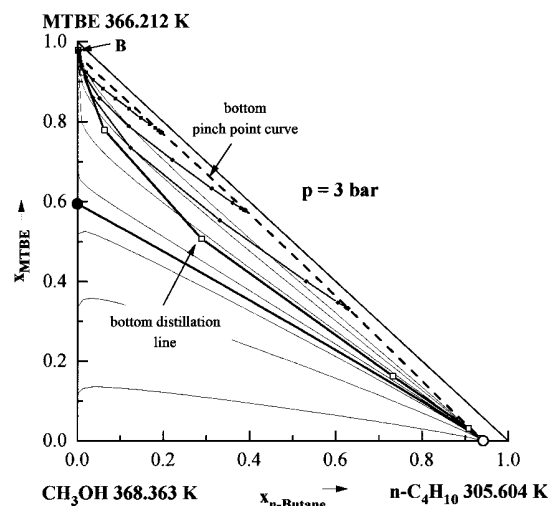


Figure 6. Region covered by the stripping profiles when the limiting reacting component is not present.

entire column, and hence, a projection onto the composition simplex of the ternary mixture between MTBE, methanol, and *n*-butane can be used to check any possible overlap of regions. Thus, the feasibility of a given separation (the column products are known) at finite values of the reflux ratio can be determined. Since the stripping and primary rectifying profiles must meet anywhere into the tetrahedron, we analyze the regions where all the possible adiabatic profiles departing from the bottom of the column and from the distillate (more precisely from the composition at the end of the reactive core) can be found.

Geometry of the Stripping Profiles. To analyze the stripping profiles the two limiting operating conditions of a column must be determined: total reflux and thermodynamically optimal operations. Let us analyze the fixed points of the finite difference equations describing the stripping section (eq 3). Fixed points are called pinch points; the collection of pinch points at different values of the boilup ratio represents the thermodynamically reversible path or bottom pinch point curve. This trajectory could theoretically be obtained in the stripping section of a column producing B with an infinite number of trays and continuous adjustment of the internal flows through boilers at each stage. Such nonadiabatic operation would be required to keep the driving forces for heat and mass transfer at a minimum throughout the stripping section (Koehler et al.⁹). With each point of that curve on the composition simplex corresponds a vapor composition in equilibrium. In addition, each of the equilibrium vectors points to the bottom composition on the concentration simplex. Hence, assuming equilibrium between the liquid and vapor compositions in eq 3, the pinch equations for the stripping section are obtained. Note that in the limiting case of total reboil, eq 3, with the liquid and vapor compositions at equilibrium, indicates that the fixed points inside the concentration simplex lie at the pure component vertexes and azeotropic compositions. Figure 6 shows the maximum area covered by the stripping profiles for the case of a bottom product without isobutene. All the adiabatic profiles are enclosed by a ternary pinch point curve and the total reflux curve (distillation line), which runs to the minimum boiling azeotrope between *n*-butane and methanol. To represent the total reflux operation, we used the distil-

lation line instead of the corresponding residue curve because the distillation line is the actual operation line for total reflux (Widagdo and Seider¹⁰). Residue curves are depicted in Figure 6 because the pinch point curve through B could be constructed by finding these points on residue curves with tangents pointing the composition of the bottom product. Since the bottom also contains traces of isobutene, it is clear that the effective region that is covered by the bottom profiles is smaller to that depicted in Figure 6. Actually, depending on the mole fraction of the lighter components, a typical profile could pass in the vicinity of a binary saddle point (MTBE–OH); then the separation proceeds into the triangular diagram limited by the components MTBE–OH–butane until a new saddle pinch is reached. The profile terminates in an inactive end pinch containing MTBE–OH–isobutene according to the theoretical explanations developed by Poellmann et al.¹¹

Geometry of the Profiles inside the Primary Rectifying Section. As can be seen in Figure 6, the calculation of the distillation line and the pinch point curve departing from the bottom composition is needed to determine the feasible region for all the adiabatic profiles in the stripping section. As it occurs in extractive distillation, a “pole” outside the tetrahedron gives rise to disjoint branches of pinch point curves which complicates the simple analysis above. Thus, a way to check feasibility is the analysis of the profile's behavior for each value of the reflux ratio. This check has to be done at least within the interval established by the minimum and maximum values of the energy demand obtained by the calculation of the pinch point curve. To do this, we must only solve the pinch equations for the primary rectifying section to identify the multiple solutions for a given value of the reflux ratio. No profiles must be calculated. A methodology to calculate pinch point curves based on homotopy continuation was presented in a previous work (Aguirre and Espinosa¹²).

As in the case for the stripping profiles, the pure component vertexes and azeotropic compositions are solutions of the pinch equations corresponding to the primary rectifying section under total reflux operation. As Knapp and Doherty³ stated in problems concerning extractive distillation, the stability of the pinch points at total reflux can be predicted from the stability of the singular points of the residue curve maps and simple temperature-based arguments. The primary rectifying section profile under total reflux operation starts at the boundary condition and moves down the column approximately following a residue curve through the boundary condition in the direction of increasing temperature until a stable point is achieved. Taking into account that the temperature always increases along each one of the distillation residue curves, the stability of fixed points in this section under total reflux coincides with that of singular points in the residue curve map. In other words, MTBE and methanol will be stable nodes both for the residue curve map and for the primary rectifying section under total reflux. In the same form, the azeotrope MTBE–alcohol and the inert will be saddles while the minimum boiling azeotrope butane–methanol will be an unstable node. The stability analysis concerning the pure limiting reagent, and the corresponding minimum boiling azeotrope is straightforward.

Depending on the location of the boundary condition under total reflux, the profile of this section will move

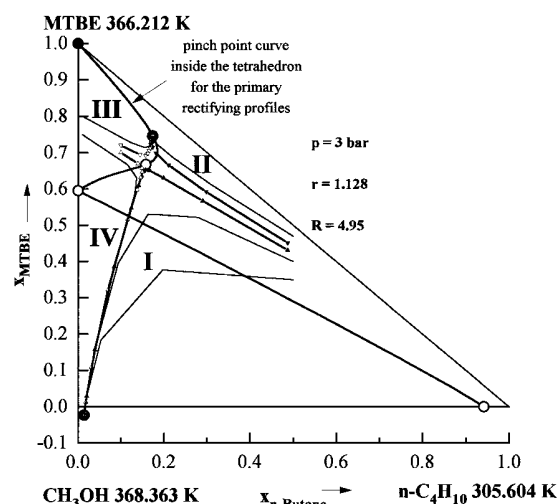


Figure 7. Primary rectifying section saddle pinch point dividing the composition state space into four regions at finite reflux.

in the direction of increasing temperature either toward pure MTBE or to pure methanol. As we have shown in the previous section, although there exists a limit for the reflux ratio in order to achieve the reaction yield, this value can be considered nearly at total reflux. Moreover, the curve of the liquid mole fractions at the end of the reactive core corresponding to Table 3 pertains to the upper section of Figure 6, and hence, we expect that at near total reflux the profiles in the primary rectifying section move to the direction of the ether. This important result shows that pure MTBE could be achieved with this topology.

At finite values of the reflux ratio, a similar analysis can be done to demonstrate that the feasibility of the separation will remain unchanged. The stability of each pinch point in this section will remain also unchanged with respect to total reflux unless a point of local or global bifurcation is found. In other words, a hypothetical pinch point curve or branch departing from the MTBE vertex will generate stable nodes for the rectifying profiles under finite reflux. On the other hand, it can be expected that a curve or branch beginning at the MTBE–methanol azeotrope will give a collection of saddle points.

Figure 7 shows how a saddle node corresponding to a given value of the reflux ratio divides the composition state space into four regions. In this figure we have calculated the tray by tray equations for different (perturbed) boundary conditions to demonstrate that depending on the location of the boundary condition, the adiabatic profile related to the given reflux ratio can terminate either in a stable pinch (containing all the components of the mixture) inside the tetrahedron or in another that lies outside the composition simplex. Each of these two points is a solution of the pinch equations at the given value of the reflux ratio. The figure shows the other solution, the saddle pinch. The stability of this point is determined by analyzing the complete pinch point curve inside the tetrahedron together with the stability at total reflux. Actually, since this point corresponds to a branch departing at total reflux from the MTBE–methanol azeotrope (a saddle for the residue curve map), it is expected that such a pinch behaves as a saddle for the primary rectifying section at finite values of the reflux ratio. A similar stability analysis can be done for the two stable nodes.

The saddle corresponding to a given reflux determines the behavior of the primary rectifying profiles because four regions into the tetrahedron are established. At the end of each line of the boundary between the four regions either stable nodes or unstable nodes can be found. Regardless of the boundary condition, the rectifying profile could be crossed by a stripping profile for the given value of the energy demand. By the analysis of Figure 7 for several values of the reflux ratio, a similar behavior can be shown. For example, under total reflux operation, the saddle coincides with the composition of the azeotrope between MTBE and methanol and the two stable nodes are MTBE and methanol, respectively. In this case, the regions marked as I and II in Figure 7 coincide with the regions at total reflux as they can be derived from the residue curve maps. As a consequence of the analysis above, the complete triangular diagram can be considered as the region for all the adiabatic profiles corresponding to the "difference point". Therefore, it can be shown that the separation of the feed into the top and a bottom compositions corresponding to the example is in principle feasible because an overlap between the top and bottom regions occurs.

As in conventional distillation, only the pinch point curves for the given distillate are necessary to sketch the behavior of the adiabatic profiles (Knapp and Doherty³). Note that all the points on the pinch curve depicted in Figure 7 point the pole as it is defined by eqs 7 and 8 ($\Delta D = [0.0664514, 0.1147230, -0.066358, 0.8851836]$, $D^* = 74.496$). The shape of the pinch curve resembles that of extractive distillation. In extractive distillation any separation at total reflux is infeasible; in this case, the separation is possible at this limit condition.

Finally, the feasible regions for the case of the feed stream located below the reactive core is enhanced with respect to the feed stream inside the reactive core. This characteristic has a positive effect on the sensitivity of the column products to changes in the operation variables for the case of MTBE production.

Minimum Energy Demand

Figure 8 shows the minimum energy demand operation in the triangular diagram. The minimum reflux situation corresponds to a value of the reflux ratio of 0.9307, and a finite number of stages is required. The liquid profiles depicted contain all the components present in the feed mixture. For this reason, these profiles are only a projection onto the triangular diagram corresponding to n -C₄H₁₀, MTBE, and CH₃OH. Note, however, that once one has calculated the boundary condition, it is possible to lump isobutene and n -C₄H₁₀ into one component inside the nonreactive section of the column below the reactive core. The point of intersection of the top and bottom profiles in Figure 8 is about 1.2 mol % isobutene.

It is noteworthy that the liquid profile in the primary rectifying section has, under minimum reflux operation, a nonactive end pinch point outside the concentration simplex. Therefore, the total reflux distillation boundary (a surface inside the tetrahedron in this case) does not act as a boundary for these profiles at finite values of the reflux ratio. Despite the behavior of the liquid profile in this zone, the intersection of the profiles pertaining to the primary rectifying and the stripping sections occurs at a tray that belongs to the upper

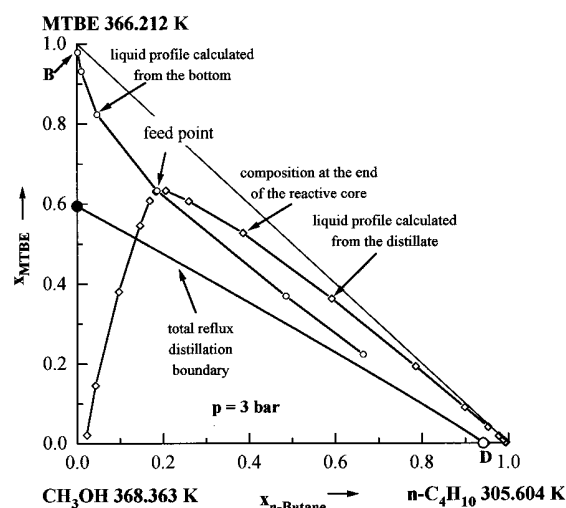


Figure 8. Shape of the profiles under minimum energy demand: projection onto the n -butane-methanol-MTBE triangular diagram. (Separation specified in Table 2.)

distillation region; i.e., the region where MTBE is the heaviest component. For this case the minimum energy demand is controlled by the reaction yield of the column. Actually, the profiles can intersect at the lower limit of the reflux ratio for which the conversion yield is achieved.

Although the distillate contains (only) two components (the other are present in traces) an end pinch for the primary rectifying section must contain the four components of the mixture because the feed to this section consists of a quaternary mixture in simultaneous chemical and physical equilibrium. In other words, the difference point consists of four components and, hence, any pinch point must contain four components. On the other hand, the bottom stream contains the two heavy species and, hence, any stripping profile must terminate in a nonactive pinch containing isobutene-methanol-MTBE. Taking the above-mentioned characteristics, we have expected a minimum reflux situation with a pinch immediately above the feed as usual in indirect separations. This apparent contradiction can be newly explained with the analysis of the pinch point curves corresponding to the difference point.

As it is known, the primary rectifying pinch point curves are the locus of fixed points as a function of the reflux ratio for the given difference point. These curves can be obtained once the distillate composition and reaction yield are fixed together with the condition of equilibrium between streams at the same height of a column that must be applied on eq 5. Each point along a pinch point curve as is shown in Figure 7 corresponds to a different value of the reflux ratio. Another way to depict the pinch point curve is the (x_{MTBE}, V) projection. Figure 9 shows that two solutions for the pinch equations are expected for values of the vapor flow rate between about 141 mol/time and infinite. The upper values correspond to stable nodes while the lower ones indicate saddles. There exists a limit point where only one solution on the pinch point curve is found. This limit point represents a typical saddle-node bifurcation because both the branches departing from MTBE and from the saddle MTBE-methanol intersect and eliminate each other at the limiting point. Primary rectifying profiles with vapor flow rates below this point will not terminate at a stable node on this pinch point curve.

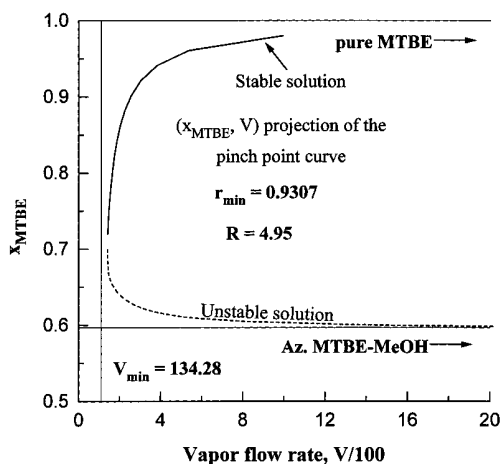


Figure 9. Fixed-point curve for a given value of the reaction yield: (x_{MTBE}, V) projection.

For this case, a profile will terminate at the pinch point curve that lies outside the tetrahedron and begin at the pure methanol vertex.

This situation occurs under minimum energy demand for the example considered. There is no pinch inside the composition simplex, and hence, the profile must be attracted for the pinch point curve that lies outside the concentration simplex. Actually, in Figure 9 there is no intersection between the line representing the minimum vapor flow rate corresponding to the rectifying profile below the reactive core and the pinch point curve.

Bifurcation of Reversible Profiles

In this section we analyze the influence of the reaction yield on the reversible profiles in the primary rectifying section of the finishing column. To do this, we suppose a feed to a hypothetical global process that includes a reactor with variable isobutene conversion. We suppose that the stream leaving the reactor is at its bubble point. Moreover we do not impose any constraint to the conversion inside the reactor; therefore, the relative conversion target could be varied between zero and one. This constraint was made to permit the analysis of the behavior of the reversible profiles along the greatest area possible and for academic purposes only. For a given design problem, the analysis must be done until the effluent from the reactor has the maximum conversion that is possible.

When the conversion target in the reactor is varied, then a change in the liquid compositions in the feed stream to the finishing column is enforced. However, all the possible feed stream compositions equal the value of the transformed mole fractions defined in eq 1 as is presented in Table 2. In addition, the same top and bottom products can be obtained in the finishing column because the balance line in the transformed model points to the same products. Only the quantity of MTBE produced in the reactive column varies. The lower the isobutene conversion in the reactor the greater the value of R/D in the column that must be achieved in order to maintain the global conversion of the entire process. This property of the transformed compositions enables us to analyze the influence of the conversion target in the column on the feasibility of a given separation and minimum reflux operation maintaining the product compositions and flows rates in the natural field at fixed values. This property of the transformed

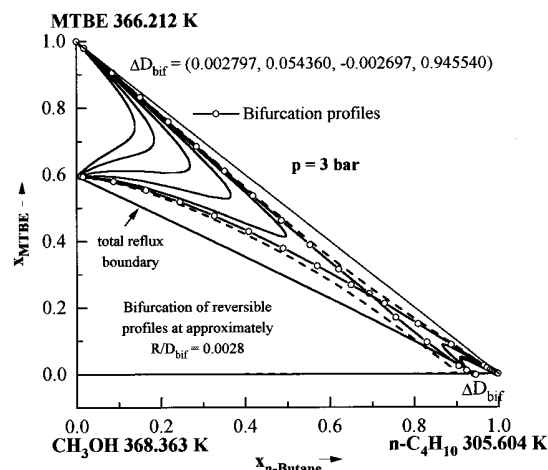


Figure 10. Shape of the reversible profiles of the primary rectifying section as a function of the ratio R/D and bifurcation profile.

model was applied in Espinosa et al.¹³ and is derived in the Appendix.

Figure 10 shows the results obtained by varying the reaction yield in the finishing column. The feed composition and molar flow rate to the hypothetical process were fixed at the following values: 120 kmol/s, [0.20795, 0.24205, 0, 0.55]. To obtain the curves in Figure 10, the isobutene conversion in the reactor should be varied between 70% and 99.5%. For all the cases, the distillate and bottom composition and flow rates remain constant. From Figure 10 it is clear that for each value of the reaction yield there exists another pinch point curve joining the representative mole fraction of the *n*-butane–methanol azeotrope and the inert vertex. As the reaction yield in the finishing column, measured as the quantity of isobutene reacted, is increased the corresponding pair of twin (pinch) curves are located farther apart from each other. In contrast, by reduction of the amount of reaction, each pair of twin curves moves closer and closer until a bifurcation of the reversible profiles take place. Under this situation, all the branches meet at a single point. This situation occurs for a value of $(R/D)_{\text{bif}}$ that equals 0.0028. The difference point coordinates are $\Delta D^*_{\text{bif}} = [0.002797, 0.054360, -0.002697, 0.945540]$. The point of intersection of the bifurcating profiles is located on a tangent to a residue curve inside the compositions tetrahedron at its point of inflection as was stated by Poellmann and Blass.¹⁴ In principle, this bifurcation point of the pinch point curve branches marks a different behavior of the profiles immediately below the reactive core depending on the value of the reaction yield. Two qualitatively different reversible profiles can appear in the primary rectifying section. These profiles differ in how the singular points of closed (total reflux) distillation are connected with reversible profile branches. For values of R/D greater than the corresponding to the bifurcation point, a pinch point curve joining pure MTBE and MTBE–methanol azeotrope are expected to influence on the behavior of the column profiles. On the other hand, for values of R/D lower than the bifurcation point, reversible profiles connecting MTBE and the inert are the curves of end points for the adiabatic profiles in the primary rectifying section. It is clear that, for the last case, the reversible profiles resemble that corresponding to a pure distillation without chemical reaction. Moreover, we can expect a minimum energy demand operation with a

pinch immediately above the feed point because the adiabatic profiles in this column section terminate at pinch points containing all the components of the feed mixture inside the tetrahedron. The end pinch corresponding to the bottom, as we have explained above, does not act under minimum reflux.

Finally, a new difference appears between extractive and reactive distillation. In extractive distillation (Wahnschafft and Westerberg;⁶ Knapp and Doherty;³ Bauer and Stichlmair⁷) the bifurcation of the reversible profiles will determine a minimum value of the entrainer flow, above which the separation is possible. In reactive distillation, the separation is also in principle possible for values of the reaction yield lower than those corresponding to the bifurcation because MTBE will remain as a stable node for the primary rectifying section under total reflux and, hence, regions rich in the ether can be achieved by these profiles at different values of the reflux ratio.

Conclusions

In this paper, a novel method for the analysis of finishing reactive distillation columns with a reactive core, two rectifying sections, and a stripping section was developed. Although the methodology was applied to a particular system, the general approach is applicable to other systems.

Geometric based methods were applied to explain some key features of quaternary reactive distillation. For a finite value of the reflux ratio a saddle divides the composition state space into four regions (see Figure 7). The primary rectifying profile can lie in any of these four zones depending on the location of the boundary condition (mole fractions and flow rate) at the end of the reactive core. For the case under consideration we demonstrated that regardless of the location of the boundary condition the rectifying profiles could be crossed by the stripping profiles for several values of the reflux ratio. The operation near total reflux is also feasible because the reaction product is a stable node of the primary rectifying section profile. This characteristic determines the key difference between the reactive distillation of mixtures, whose reaction product remains as a stable node under total reflux operation, and extractive distillation.

Extractive distillation always presents a maximum value for the energy demand above which the separation is infeasible. This value depends on the amount of entrainer used for the separation. Another characteristic appears in reactive distillation: a finite number of trays in each section of the column is needed under minimum reflux whenever the minimum operation reflux for which the bottom and top profiles intersect is lower than that corresponding to the saddle-node bifurcation (see Figure 9). The value corresponding to the saddle-node bifurcation depends here on the value of the reaction yield determined through the overall balances.

Finally, the behavior of the adiabatic profiles depends on the ratio R/D because a bifurcation of the reversible profiles is possible in finishing columns (see Figure 10). Newly, a difference appears between reactive distillation and extractive distillation. For values of the entrainer flow rate below the bifurcation point, the separation is infeasible for all values of the reflux ratio. On the other hand, we expect feasible designs for reactive columns whose ratio R/D is lower than that corresponding to the

bifurcation of reversible profiles. The reason is that the reaction product remains as a stable node for the primary rectifying profile under total reflux. Minimum energy demands with pinch (infinite number of trays) are expected for this case just above the feed because the pinch curves resemble that of nonreactive distillation.

As for nonideal distillation, geometric based methods are very powerful to understand the key features of reactive distillation and must be used at the first step of the design and synthesis.

Acknowledgment

J.E. gratefully acknowledges the financial support of DAAD (Deutscher Akademischer Austauschdienst) of the work reported here. P.A. thanks DAAD and UNL (Universidad Nacional del Litoral, Argentina). Both authors are also grateful to Prof. Dr.-Ing. Johann Stichlmair for the kind hospitality and motivating work environment provided during this work.

Nomenclature

I = inert
 B = bottom, bottom molar flow rate (kmol/s)
 D = distillate, distillate molar flow rate (kmol/s)
 F = feed stream, feed stream flow rate (kmol/s)
 L = internal liquid molar flow rate (kmol/s)
 N = number of the column trays, total number of moles
 n_c = number of components
 p = column pressure (bar)
 R = reaction yield (kmol/s)
 r = reflux ratio
 s = reboil ratio
 V = internal vapor molar flow rate (kmol/s)
 x_j = molar fraction of component j in the liquid phase
 X_j = transformed composition of component j in the liquid phase
 y_j = molar fraction of component j in the vapor phase
 Y_j = transformed composition of component j in the vapor phase
 $I-IV$ = zones of the composition state space generated by a saddle pinch

Greek Letters

ξ = extent of reaction
 ν_j = stoichiometric coefficient of component j
 ν_t = sum of the stoichiometric coefficients of the reacting species

Subscripts

I = inert
 II = denotes the primary rectifying section
 B = bottom
 bif = bifurcation
 D = distillate
 m = generic tray above the feed tray
 min = minimum
 n = generic tray below the feed tray, index for the number of trays
 $stripping$ = stripping section

Superscripts

$*$ = transformed value
 0 = initial condition
 f = final condition

new = denotes the new transformed distillate mole fraction or difference point

Appendix

The feed to the ideal reactor considered in this paper has an initial composition in the transformed field that remains constant after the reaction. Therefore, the transformed composition of the feed to the column equals that of the feed to the global process. The same occurs for the transformed mole flow rate as is defined in previous works. We suppose that the feed to the finishing column is at its bubble point.

The total number of moles of each component that are present in the feed to the column are given by (we have eliminated the time variable for the sake of simplicity)

$$N_j^f = N_j^0 + \nu_j \xi \quad (\text{A1})$$

for the reacting species. The total number of moles of the inert remains constant at a value of

$$N_I^f = N_I^0 \quad (\text{A2})$$

The variable ξ represents the extent of the reaction inside of the reactor. In the same form, the liquid mole fractions of the feed to the column are defined in terms of the mole fractions of the feed to the reactor, their total number of moles and the extent of reaction ξ as

$$x_j^f = \frac{x_j^0 + \nu_j \frac{\xi}{N_0}}{1 + \nu \frac{\xi}{N_0}} \quad (\text{A3})$$

for the reacting components. The liquid mole fraction for the inert can be expressed as

$$x_I^f = \frac{x_I^0}{1 + \nu \frac{\xi}{N_0}} \quad (\text{A4})$$

Applying eqs 1 to obtain the transformed mole fraction for the feed to the finishing column it is straightforward to demonstrate that the transformed mole fractions have the same value before and after the reaction step:

$$X_j^f = X_j^0 \quad (\text{A5})$$

As a consequence of equality (A5), we can model the situation described in the main body of the paper.

Literature Cited

- (1) Bessling, B.; Schembecker, G. and Simmrock, K. H. Design of Processes with Reactive Distillation Line Diagrams. *Ind. Eng. Chem. Res.* **1997**, *36*, 3032–3042.
- (2) Espinosa, J.; Aguirre, P. and Pérez, G. Some Aspects in the Design of Multicomponent Reactive Distillation Columns with a Reacting Core: Mixtures Containing Inerts. *Ind. Eng. Chem. Res.* **1996**, *35*, 4537–4549.
- (3) Knapp, J. P.; Doherty, M. F. Minimum Entrainer Flows for Extractive Distillation: A Bifurcation Theoretic Approach. *AIChE J.* **1994**, *40*, 0 (2), 243–268.
- (4) Espinosa, J.; Aguirre, P.; Pérez, G. Some Aspects in the Design of Multicomponent Reactive Distillation Columns Including Non Reactive Species. *Chem. Eng. Sci.* **1995(a)**, *50* (3), 469–484.
- (5) Espinosa, J.; Aguirre, P.; Pérez, G. The Product Composition Regions of Single-Feed Reactive Distillation Columns: Mixtures Containing Inerts. *Ind. Eng. Chem. Res.* **1995 (b)**, *34*, 853–861.
- (6) Wahnschafft, O. M.; Westerberg, A. W. The Product Composition Regions of Azeotropic Distillation Columns. 2. Separability in Two-Feed Columns and Entrainer Selection. *Ind. Eng. Chem. Res.* **1993**, *32*, 1108–1120.
- (7) Bauer, M. H.; Stichlmair, J. Synthesis and Optimization of Distillation Sequences for the Separation of Azeotropic Mixtures. *Comput. Chem. Eng.* **1995**, *19*, S15–S20.
- (8) Wahnschafft, O. M.; Koehler, J.; Blass, E.; Westerberg, A. W. The Product Composition Regions of Single-Feed Azeotropic Distillation Columns. *Ind. Eng. Chem. Res.* **1992**, *31*, 2345–2362.
- (9) Koehler, J.; Aguirre, P.; Blass, E. Minimum Reflux Calculations for Nonideal Mixtures Using the Reversible Distillation Model. *Chem. Eng. Sci.* **1991**, *46* (12), 3007–3021.
- (10) Widagdo, S.; Seider, W. D. Azeotropic Distillation. *AIChE J.* **1996**, *42* (1), 96–130.
- (11) Poellmann, P.; Glanz, S.; Blass, E. Calculating Minimum Reflux of Nonideal Multicomponent Distillation using Eigenvalue Theory. *Comput. Chem. Eng.* **1994**, *18*, S49–S53.
- (12) Aguirre, P. A., and Espinosa, J. A Robust Method to Solve Mass Balances in Reversible Column Sections. *Ind. Eng. Chem. Res.* **1996**, *35*, 559–572.
- (13) Espinosa, J.; Scenna, N.; Pérez, G. Graphical Procedure for Reactive Distillation Systems. *Chem. Eng. Commun.* **1993**, *119*, 109–124.
- (14) Poellmann, P. and Blass, E. Best Products of Homogeneous Azeotropic Distillations. *Gas Sep. Purif.* **1994**, *8* (4), 193–227.

Received for review October 6, 1997

Revised manuscript received September 11, 1998

Accepted September 14, 1998

IE9707073